Quasi-LPV Interconnected Observer Design for Full Vehicle Dynamics Estimation With Hardware Experiments

Majda Fouka, Chouki Sentouh, Jean-Christophe Popieul

Quasi-LPV Interconnected Observer Design for Full Vehicles Dynamics Estimation with Hardware Experiments

M. Fouka, C. Sentouh, *Member, IEEE,* J-C. Popieul

***Abstract*—Safety systems claim an in-depth study of vehicle motion and tire-ground interaction for the design of the partially automated driving vehicle. This paper addresses the quasi-linear parameter-varying (Quasi-LPV) Luenberger Interconnected Fuzzy (QLIF) observer to estimate simultaneously both longitudinal and lateral vehicle dynamics. In a different manner from the commonplace state-of-the-art of vehicle state observers that consider the single driving motion, the proposed approach considers the coupled dynamics with tire-ground interaction to estimate the most important states while reducing the complexity related to the observability and conservatism. This consideration leads to a nonlinear parameter-dependent interconnected model with unmeasured premise variables. Then, the Takagi-Sugeno (TS) fuzzy form is considered to deal with the nonlinearities of the vehicle longitudinal and lateral speeds and the slip velocities as well as the steering angle. The concept of "Input to State Stability (ISS)" is exploited using fuzzy non-quadratic Lyapunov stability arguments to guarantee the boundness of the estimation errors. A refinement has been proposed through the so-called Polya's theorem aiming to reduce further the conservativeness. Finally, the performances and effectiveness of the suggested approach are evaluated through hardware experiments performed with the well-known SHERPA dynamic car simulator under real-world driving situations.**

***Index Terms*—Vehicle Safety, longitudinal and lateral dynamics, Quasi-LPV Interconnected Observer, ISS Stability.**

I. INTRODUCTION

The involvement of autonomous ground vehicles in the daily life transportation has attracted the attention of industrial and research laboratories around the world to face the new arising challenges. In this context, the integration of Advanced Driver Assistance Systems (ADAS) for autonomous ground vehicle is one of the forward objectives of automakers and suppliers, to help make partially or completely automated driving, which may highly affect the global vehicle economy. Among others, vehicle state estimation have been largely investigated with a growing body of literature for observer design [1]. This topic is one of our research interest which intends to develop ADAS systems starting from a minimum set of vehicle self-integrated sensors. Virtual sensor and observers approaches are widely proposed from onboard-sensor to develop theoretical tools solving many safety problems, such as, lateral dynamics estimation in [2], reconstruction of vehicle-road interaction to improve the vehicle performance for comfort and safety from sliding mode approach in [3], tire longitudinal forces from adaptive neural network observer in [4]. Recently, the simultaneous estimation of lateral dynamics and driver's torque proposed using unknown input observers (UIO) in [5] deploying either LPV techniques or the Takagi-Sugeno transformation. Moreover, vehicle characteristics and road conditions may change for different driving situations. In [6], non-linear UIO are applied to lateral dynamics estimation on banked or slop roads. The cornering stiffness identification is considered with adaptive observer in [7]. Further, in [8], a closed-loop cascade control architecture with interconnected pressure estimation for a brake system is proposed with an experimental validation demonstrating excellent tracking performance and robustness. To deal with motorcycle lateral and longitudinal dynamics, a convenient interconnected approach has been investigated in [9] using motorcycle software evaluation. In [10], the authors proposed a cascade decoupled observer structure to enable the estimation of vertical and lateral forces from each independent observer. Almost references, the estimation of the vehicle dynamics is done by considering restrictive assumptions regarding driving scenario, independent or decoupled behavior or under a constant speed, tire-road contact has often been neglected. These assumptions simplify the estimation problem but, it may lead to an inaccurate reconstruction with respect to the real dynamics. Starting from these points and keeping in mind the reduction of vehicle sub-models, it is a natural and orderly way of viewing the global vehicle systems as being composed of two lower order subsystems which, when linked in an appropriate fashion, yield to interconnected coupled system. In particular, this interconnection has a physical meaning, it can represent a pure motion when only the lateral or longitudinal dynamics are excited, each of which being in charge of a local control/observation/supervision/FDI/FTC unit or it could result from different ADAS objectives. Also, it is notably attractive to suppress the propagation of a disturbance within an interconnection of subsystems [11]. Overall, the proposed approach is inspired by the theoretical technique originally exposed for motorcycles in [9], which is extended to provide practical conditions with less conservatism with realistic validation, to give a generalized use for the vehicle interconnected-observer.

This research was funded by the European Union with the European Regional Development Fund, the French State and the Hauts-de-France Region under the project VUMOPE-ELSAT 2020. This work has been done also within the framework of the CoCoVeIA project (ANR-19-CE22-0009-01) funded by the Agence Nationale de la Recherche, the Ministry of Higher Education and Research and the French National Center for Scientific Research.
M. Fouka is with the Univ. Polytechnique Hauts-de-France, LAMIH, CNRS, UMR 8201, F-59313 Valenciennes, France. C. Sentouh and J-C. Popieul are with the Univ. Polytechnique Hauts-de-France, LAMIH, CNRS, UMR 8201, F-59313 Valenciennes, France, INSA Hauts-de-France, F-59313 Valenciennes, France. E.mail: majda.fouka@uphf.fr

Herein, we are interested in both lateral and longitudinal coupled nonlinear vehicle dynamics estimation using a Quasi-LPV Luenberger Interconnected Fuzzy Observer (QLIF). The main contributions are summarized in the following items:

1- Reconsider the luenberger observer synthesis for a vehicle interconnected system with unknown non linearities related to forward and lateral speeds and slip velocities at the front and rear tires as well as the measured steer angle. Novel QLIF structure overcomes the mutual dependence and reduces conservativeness in the optimization scheme.
2- Relaxed stability conditions of the observer by deploying Fuzzy non-quadratic Lyapunov function through the use of slack variables and the Polya's theorem [12].
3- The influence of the immeasurable premise variables and the robustness proof with respect to modeling uncertainties and additive bounded perturbations are explored according to the ISS concept.
4- The effectiveness is highlighted using a "full scale" SHERPA car simulator under real-world driving situation with robustness test performed regarding noises, road friction changes and parameters uncertainties.

The document is organized as follow: Section II deals with the lateral and longitudinal models of the vehicle and the tire-ground forces dynamics; while the third section presents the model through the TS fuzzy form. The fourth section presents the design of QLIF observer. The fifth section is devoted to the simulations and analysis of the results. Finally, the conclusion is given in the last section.

II. Complete Interconnected Vehicle Dynamics

In the following, we are concerned by a nonlinear coupling vehicle model with 9-DoF (nine degrees of freedom), which includes longitudinal, lateral, yaw motions, rotational movements of the two wheels and the tire longitudinal and cornering forces dynamics of the front/rear wheels.

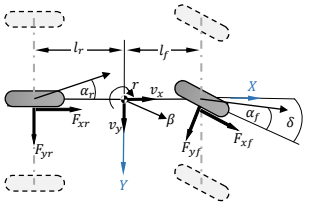

Fig. 1: Bicycle Model.

A. Vehicle Lateral Dynamics Description

The nonlinear lateral dynamics of the vehicle is represented as a bicycle model Fig. 1, widely used, which have only planar motion parallel to the road's surface [13]. We assume that the vertical, pitch, and roll dynamics are neglected. This representation describes the lateral dynamics: by body-fixed yaw motion $\dot{\psi}$ and the lateral speed v_y, with the following equations

$$\begin{cases} m\dot{v}_y = F_{xf}\sin(\delta) + F_{yf}\cos(\delta) + F_{yr} - mv_x\dot{\psi} - C_y v_y^2 \\ I_z\ddot{\psi} = l_f F_{yf}\cos(\delta) - l_r F_{yr} + l_f F_{xf} sin(\delta) \end{cases} \quad (1)$$

B. Tire Forces Dynamics

In literature, the Pacejka model is the most widespread including tire saturation [13]

$$F_i(\nu) = D_i sin(C_i tan^{-1}(B_i(1-E_i)\nu_i + E_i tan^{-1}(B_i\nu_i))) \quad (2)$$

- $i = \{r, f\}$ denotes rear and front of the vehicle;
- D_i, C_i, B_i and E_i: pneumatic intrinsic characteristics.
- ν is a generic variable which corresponds to the side-slip angle α or the longitudinal slip ratio λ.

$$\alpha_f = \delta - \frac{v_y + l_f\dot{\psi}}{v_x} \quad \text{and} \quad \alpha_r = -\frac{v_y - l_r\dot{\psi}}{v_x}$$
$$\lambda_f = (R\omega_f - v_x)\varrho_f \quad \text{and} \quad \lambda_r = (R\omega_r - v_x)\varrho_r \quad (3)$$

$\varrho_i = \frac{1}{max\{v_x, R\omega_i\}}$ is the nonlinear slip velocity. In order to quantify the sliding proportion on braking and traction motions, the nonlinear slip velocity ϱ_i is considered as a switching varying parameter expressed as

$$\varrho(t) = \begin{cases} \varrho_i = \frac{1}{\omega_i R} & \lambda_i > 0 \quad \text{if Traction :} \quad v_x < \omega_i R \\ \varrho_i = \frac{1}{v_x} & \lambda_i < 0 \quad \text{if Braking :} \quad v_x > \omega_i R \end{cases} \quad (4)$$

The ϱ_i are assumed to be unknown but bounded with a priori known bounds. In control problems, the Pacejka model is cumbersome. For small values of α or λ, the lateral F_y and longitudinal F_x forces can be approximated by a linear model

$$F_y = C_\alpha\alpha \quad \text{and} \quad F_x = C_\lambda\lambda \quad (5)$$

The Pacejka formula or its linear form describe only the static behavior. However, due to its elastic deformation, a transient behavior occurs. Almost literature includes a first order low-pass filter $\tau_i = \frac{\sigma_i}{v_x}$ to model the transient behavior [14] as

$$\frac{\sigma_y}{v_x}\dot{F}_y = -F_y + F_y^0 \quad \text{and} \quad \frac{\sigma_x}{v_x}\dot{F}_x = -F_x + F_x^0 \quad (6)$$

F_x^0 and F_y^0 are the steady-state value obtained from magic formula (2) or the linear form (5), (σ_i) is the relaxation lengths.

C. Mathematical Model of Longitudinal Vehicle Dynamics

To consider the longitudinal dynamics, the wheel's rotational movements $\omega_{(f,r)}$ including the traction and braking motions and the longitudinal displacement are modeled

$$\begin{cases} m\dot{v}_x = F_{xf}\cos(\delta) - F_{yf}sin(\delta) + F_{xr} + mv_y\dot{\psi} - C_x v_x^2 \\ i_{fy}\dot{\omega}_f = -RF_{xf} + T_f + B_f \\ i_{ry}\dot{\omega}_r = -RF_{xr} + B_r \end{cases} \quad (7)$$

All variables are defined in Table II.

III. LPV polytopic form of Vehicle System

Using the sector nonlinearity [15], the lateral and the rectilinear motions with tire forces (1), (6) and (7) are linked in interconnected form with its q varying parameters exactly rewritten as a compact TS representation with $r = 2^q$ linear sub-models weighted by membership functions $\mu_i(\vartheta_k)$ depending on the immeasurable state variables. These latter satisfy the convex-sum property

$$0 \le \mu_i(\vartheta_k) \le 1, \ \sum_{i=1}^{r}\mu_i(\vartheta_k) = 1, \ \text{and} \ \sum_{i=1}^{r}\dot{\mu}_i(\vartheta_k) = 0 \quad (8)$$

and ϑ_k: $(k = \{x, y\})$, called premise variables, are the judged vectors of varying parameters in the longitudinal and lateral models. The bounds of these smooth scheduling variables $\vartheta_k \in \mathcal{R}^q$ are defined in an hyper-rectangles Θ given by

$$\Theta : \left\{\vartheta_{k_i} \in \mathbb{R}^q |\ \vartheta_{k_i}^{\min} \le \vartheta_{k_i} \le \vartheta_{k_i}^{\max}\ \right\} \quad (9)$$
$$k = \{x, y\} \quad \text{and} \quad i = \{1, .., q\}$$

where $\vartheta_{k_i}^{\min}$ and $\vartheta_{k_i}^{\max}$ are known lower and upper bounds on ϑ_{k_i}, for $i = \{1, .., q\}$ premise variable, applied for each motions $k = \{x, y\}$ and q is the number of non-linearities for each sub-system. The conservatism problem is usually induced by a judge number of vertexes ϑ_k in the polytop. Hence, an adequate choice of the nonlinearities is desirable for reducing the numerical complexity. Inspired from [16], the information on the vehicle speed bounds and the relation between v_x, $\frac{1}{v_x}$ and $\frac{1}{v_x^2}$ are exploited through the use of the following variable change and Taylor's series expansion

$$\frac{1}{v_x} = \frac{1}{v_0} + \frac{1}{v_1}\Delta_v, \quad v_x \approx v_0\left(1 - \frac{v_0}{v_1}\Delta_v\right), \quad \frac{1}{v_x^2} = \frac{1}{v_0^2}(1 + 2\frac{v_0}{v_1}\Delta_v)$$

The new unmeasured time-varying parameter $\Delta_v(t)$ describes the variation of v_x between its lower and upper bounds. This new parameter verifies $\Delta_v^{min} \leq \Delta_v \leq \Delta_v^{max}$, $\Delta_v^{min} = -1$, and $\Delta_v^{max} = 1$. The two constants v_0 and v_1 are given by

$$v_0 = \frac{2\vartheta_{\min}\vartheta_{\max}}{\vartheta_{\max} + \vartheta_{\min}}, v_1 = \frac{2\vartheta_{\min}\vartheta_{\max}}{\vartheta_{\min} - \vartheta_{\max}}, \tag{10}$$

Note that the interconnected vehicle dynamics depends on the unmeasured and bounded varying parameters namely the speed variation parameters Δ_v, the nonlinear slip velocities ϱ_f, ϱ_r on the front and rear wheels and the lateral speed v_y as well as the measured steering angle nonlinearities.

Remark 1. In classical TS Polytopic framework, conservatism problem is usually caused by the large number of sub-models. Consequently, when the number of varying parameters increases the number of LMI increases, which leads to computational complexity solving. To avoid this inconvenience, we express the system as an interconnected system to have less number of verticies and to reduce the conservatism in the observers structure. This problem has been dealt with by different approaches. As demonstrated in [12], the descriptor representation can significantly reduce the LMIs conservativeness by keeping the descriptor structure rather than classical state space form, thus, it may increase the feasibility set. Considering the interlinked models separately taken in the LMI optimization with $\vartheta_x = [\Delta_v, sin(\delta), cos(\delta), \varrho_f, \varrho_r]^T \in R^5$ leads to $r = 2^5 = 32$ LTI longitudinal submodels and $\vartheta_y = [\Delta_v, \sin(\delta), cos(\delta), v_y]^T \in R^4$ leads to $r = 2^4 = 16$ LTI lateral submodels. However, if we consider the global system with $\vartheta = [\Delta_v, \sin(\delta), cos(\delta), v_y, \varrho_f, \varrho_r]^T \in R^6$ is the global polytope vector, this leads to $r = 2^6 = 64$ sub-models and consequently to 64 LMIs. Comparing with the global model, the interconnected solution can be very useful to guarantee a less conservative design and a reduced complexity.

The lateral and the rectilinear motions with tire forces (1), (6) and (7) are transformed into a Quasi-LPV interconnected system modelled in the following equivalent TS form

$$\begin{cases} \dot{\xi} = \begin{bmatrix} \bar{A}_\mu & 0 \\ 0 & \breve{A}_\mu \end{bmatrix}\xi + \begin{bmatrix} \bar{B}_\mu & 0 \\ 0 & \breve{B}_\mu \end{bmatrix}u + \begin{bmatrix} 0 & \bar{D}_\mu \\ \breve{D}_\mu & 0 \end{bmatrix}\xi \\ y = \begin{bmatrix} \bar{C} & 0 \\ 0 & \breve{C} \end{bmatrix}\xi, \end{cases} \tag{11}$$

where: $\xi(t) = [\xi_1(t)\ \xi_2(t)]^T$, $u(t) = [u_B(t)\ u_\delta(t)]^T$, $y(t) = [\bar{y}(t)\ \breve{y}(t)]^T$ are the states, the inputs and the outputs vectors of the interconnected subsystems. With $\xi_1(t)$ refers to $[v_x, \omega_f, \omega_r, F_{xf}, F_{xr}]^T$, and $\xi_2(t) = [v_y, \dot{\psi}, F_{yf}, F_{yr}]^T$ represent respectively the state vectors for the longitudinal ($\sum_x$) and the lateral ($\sum_y$) dynamics, the control inputs of subsystems ($\sum_x$) and ($\sum_y$) are $u_B = [B_f + T_f,\ B_r]^T$ and $u_\delta = \delta$. Also, $\bar{y} = [\omega_f, \omega_r, a_x]^T$, and $\breve{y} = [\dot{\psi}, a_y]^T$ represent the output vector for each model. With ($\bar{D}_\mu$, $\breve{D}_\mu$) are the coupling matrices in the interconnection scheme.

$$\bar{A}_\mu = \sum_{i=1}^{r}\mu_i(\vartheta_x)\bar{A}_i, \quad \bar{B}_\mu = \sum_{i=1}^{r}\mu_i(\vartheta_x)\bar{B}_i, \quad \bar{D}_\mu = \sum_{i=1}^{r}\mu_i(\vartheta_x)\bar{D}_i$$

$$\breve{A}_\mu = \sum_{i=1}^{r}\mu_i(\vartheta_y)\breve{A}_i, \quad \breve{B}_\mu = \sum_{i=1}^{r}\mu_i(\vartheta_y)\breve{B}_i, \quad \breve{D}_\mu = \sum_{i=1}^{r}\mu_i(\vartheta_y)\breve{D}_i$$

where matrices $\bar{A}_i$, $\breve{A}_i$, $\bar{B}_i$, $\breve{B}_i$, $\bar{D}_i$ and $\breve{D}_i$ are constant for all $i \in [1, ..., r]$ and $r = 2^{q_x}$ for longitudinal and $r = 2^{q_y}$ for lateral subsystem with $q_y = 4$ and $q_x = 5$.

IV. Observer Design

In the sequel, the objective is to design a quasi-LPV Luenberger interconnected Fuzzy observer (QLIF) with state dependent matrices and immeasurable premise variables.The QLIF observer is based on the interconnection between two Luenberger sub-observers. An overall of the estimation scheme is depicted in Fig. 2. Stability analysis is conducted by employing the ISS based-parameter dependent Lyapunov candidate to reduce the conservativeness.

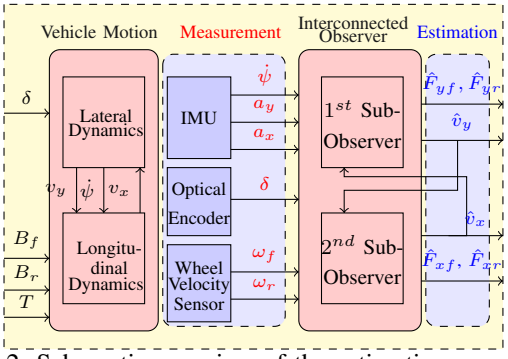

Fig. 2: Schematic overview of the estimation approach.

Assumption 1.

(i) (ξ_1) and (ξ_2) are bounded: stable or stabilized motion;
(ii) Suppose that (u_B) and (u_δ) are known and bounded.
(iii) Assume that, each sub-observer exchange some informations through the interconnection scheme.
(iiii) ($\breve{A}_\mu, \breve{C}$) and ($\bar{A}_\mu, \bar{C}$) are observable or detectable.

For observer design, the first assumption holds in open-loop and the vehicle remain in a bounded state-space region to guarantee stability. It is also assumed that normal drivers can be expected capable of maintaining a stable vehicle motion (Assumption ii). By assumption (iii), we mean that the estimator request current state information from the neighboring subsystems through the interconnection as it is the case of the vehicle motions because of the physical interactions. The last assumptions can easily be checked numerically.

A. State estimation

In this paper, we are particularly interested in designing fuzzy Luenberger-type structure inspired from [17] which relaxes some difficulties due to its particular structure and provides extra degrees of freedom [18], [5] to get directly

LMIs constraints instead of BMIs stability conditions. The overall QLIF observer, in the TS form

$$\begin{aligned}\dot{\hat{\xi}} &= \begin{bmatrix} \bar{A}_{\hat{\mu}} & 0 \\ 0 & \breve{A}_{\hat{\mu}} \end{bmatrix}\hat{\xi} + \begin{bmatrix} \bar{B}_{\hat{\mu}} & 0 \\ 0 & \breve{B}_{\hat{\mu}} \end{bmatrix}u + \begin{bmatrix} 0 & \bar{D}_{\hat{\mu}} \\ \breve{D}_{\hat{\mu}} & 0 \end{bmatrix}\hat{\xi} \\ &+ \begin{bmatrix} P_{\hat{\mu}}^{-1}\bar{L}_{\hat{\mu}} & 0 \\ 0 & Q_{\hat{\mu}}^{-1}\breve{L}_{\hat{\mu}} \end{bmatrix}(y-\hat{y}) \\ \hat{y} &= \begin{bmatrix} \bar{C} & 0 \\ 0 & \breve{C} \end{bmatrix}\hat{\xi} \end{aligned} \tag{12}$$

Where : $\hat{\xi}(t) = [\hat{\xi}_1(t)\ \hat{\xi}_2(t)]^T$ are the estimated states vector and $\hat{y}(t) = [\hat{\bar{y}}(t)\ \hat{\breve{y}}(t)]$ are the output vectors. $\hat{\mu}$ are the estimated weighting functions. The observer's matrices ($\bar{L}_{\hat{\mu}}$ and $\breve{L}_{\hat{\mu}}$) and the symmetric positive definite matrices ($P_{\hat{\mu}}$ and $Q_{\hat{\mu}}$) are parameter varying with the same quasi-LPV form as the matrices $\bar{A}_{\mu}$ and $\breve{A}_{\mu}$. Let's denote the observers errors $e_{\xi}(t) = [e_{\xi_1}^T(t)\ \ e_{\xi_2}^T(t)]^T = [\xi_1 - \hat{\xi}_1, \xi_2 - \hat{\xi}_2]^T$. According to the observer equations (12) and the system dynamics (11), the estimation errors obey the differential equation

$$\dot{e}_{\xi} = \begin{bmatrix} \bar{\Phi}_{\hat{\mu}} & \bar{D}_{\hat{\mu}} \\ \breve{D}_{\hat{\mu}} & \breve{\Phi}_{\hat{\mu}} \end{bmatrix} \times e_{\xi} + \begin{bmatrix} \Delta_{\xi_1} \\ \Delta_{\xi_2} \end{bmatrix} \tag{13}$$

$$\begin{aligned} \bar{\Phi}_i &= \bar{A}_i - P_{\hat{\mu}}^{-1}\bar{L}_i\bar{C} \quad \breve{\Phi}_i = \breve{A}_i - Q_{\hat{\mu}}^{-1}\breve{L}_i\breve{C} \\ \Delta_{\xi_1} &= (\bar{A}_{\mu} - \bar{A}_{\hat{\mu}})\xi_1 + (\bar{B}_{\mu} - \bar{B}_{\hat{\mu}})u_B + (\bar{D}_{\mu} - \bar{D}_{\hat{\mu}})\xi_2 \\ \Delta_{\xi_2} &= (\breve{A}_{\mu} - \breve{A}_{\hat{\mu}})\xi_2 + (\breve{B}_{\mu} - \breve{B}_{\hat{\mu}})u_{\delta} + (\breve{D}_{\mu} - \breve{D}_{\hat{\mu}})\xi_1 \end{aligned} \tag{14}$$

Remark 2. According to assumption 1, the state vector $\xi(t)$ is stable and, since the weighting functions μ_i in (8) are positive and convex, then the terms $\Delta_{\xi_i}(t)$ are also bounded. Hence, the estimation problem is reduced to determine the observer gains ($\bar{L}_i$, $\breve{L}_i$), and ($P_{\hat{\mu}}$, $Q_{\hat{\mu}}$) such that the estimation errors $e_{\xi}(t)$ have an asymptotic convergence towards zero if $\Delta_{\xi_i}(t) = 0$, and to ensure an ISS property when $\Delta_{\xi_i}(t) \neq 0$.

Definition 1. [9] The state estimation error dynamics verifies the ISS if there exists a $\mathcal{KL}$ function $f_1 : \mathbb{R}^n \times \mathbb{R} \longrightarrow \mathbb{R}$, a $\mathcal{K}$ function $f_2 : \mathbb{R} \longrightarrow \mathbb{R}$ such that for each input $\xi(t)$ satisfying $\|\Delta(t)\|_{\infty} < \infty$ and each initial conditions $e(0)$, the trajectory of the error associated to $e(0)$ and $\Delta(t)$ satisfies

$$\|e(t)\|_2 \leq f_1\left(\|e(0)\|, t\right) + f_2\left(\|\Delta(t)\|_{\infty}\right) \tag{15}$$

Lemma 1. [7] Consider S and R matrices with appropriate dimensions. For every matrix $\Lambda > 0$, the property holds

$$S^T R + R^T S \leq S^T \Lambda S + R^T \Lambda^{-1} R \tag{16}$$

B. Stability & Convergence Analysis of the QLIF Observer

The following theorem 1 states the first main result of this paper by ensuring an estimation of the state vectors.

Theorem 1. Provided the polytopic system (11) under stated assumptions with an ISS stability of the estimation errors. If there exist two symmetric positive definite matrices $P_{\hat{\mu}}$ and $Q_{\hat{\mu}}$, two symmetric matrices P_0 and Q_0, two positive scalars $\bar{\mathcal{M}}_i$ and $\breve{\mathcal{M}}_i$ upper bounds of the weighting functions derivatives, two diagonal positive definite matrices Ω_1 and Ω_2, and positive scalars η_1, η_2, given two positive definite matrices $\bar{R}_i$ and $\breve{R}_i$, a positive scalars γ, χ_1, $\alpha > 0$ and $a \in [0, 1]$ and gains matrices $\bar{L}_i$ and $\breve{L}_i$, $\ i = 1, ..., r$ solutions of the following LMI optimization problem

$$\min_{P_i, Q_i, P_0, Q_0, \eta_1, \eta_2} \quad a\eta_1 + (1-a)\eta_2 \tag{17}$$

under the constraints

$$\begin{cases} P_i + P_0 \geq 0, Q_i + Q_0 \geq 0, i = 1, ..., r \\ \bar{\Pi}_{ii} < 0, \breve{\Pi}_{ii} < 0, \\ \bar{\Pi}_{ii} + \bar{\Pi}_{ij} + \bar{\Pi}_{ji} < 0, j \neq i \\ \breve{\Pi}_{ii} + \breve{\Pi}_{ij} + \breve{\Pi}_{ji} < 0, j \neq i \\ \bar{\Pi}_{ij} + \bar{\Pi}_{ji} + \bar{\Pi}_{ik} + \bar{\Pi}_{ki} + \bar{\Pi}_{jk} + \bar{\Pi}_{kj} < 0, \\ \breve{\Pi}_{ij} + \breve{\Pi}_{ji} + \breve{\Pi}_{ik} + \breve{\Pi}_{ki} + \breve{\Pi}_{jk} + \breve{\Pi}_{kj} < 0, \\ j \neq i, i \neq k, j \neq k \end{cases} \tag{18}$$

where Π_{ij} are defined by

$$\bar{\Pi}_{ij} = \begin{bmatrix} \bar{A}_i^T P_j + P_j \bar{A}_i - \bar{L}_i\bar{C} - \bar{C}^T\bar{L}_i^T + \Omega_2 + \alpha P_j + P_{\bar{\mathcal{M}}} & P_j\bar{D}_i + \bar{R}_i \\ \bar{D}_i^T P_j + \bar{R}_i^T & -\Omega_1 \end{bmatrix} < 0 \tag{19a}$$

$$\breve{\Pi}_{ij} = \begin{bmatrix} \breve{A}_i^T Q_j + Q_j \breve{A}_i - \breve{L}_i\breve{C} - \breve{C}^T\breve{L}_i^T + \Omega_1 + \alpha Q_j + Q_{\breve{\mathcal{M}}} & Q_j\breve{D}_j + \breve{R}_i \\ \breve{D}_j^T Q_j + \breve{R}_i^T & -\Omega_2 \end{bmatrix} < 0 \tag{19b}$$

$$\begin{pmatrix} \gamma\eta_1 I & P_i \\ P_i & \gamma\eta_1 I \end{pmatrix} > 0, \begin{pmatrix} \gamma\eta_2 I & Q_i \\ Q_i & \gamma\eta_2 I \end{pmatrix} > 0, \mathcal{Q}_i \geq \chi_1 I \tag{19c}$$

and $P_{\bar{\mathcal{M}}} = \sum_{i=1}^{r} \bar{\mathcal{M}}_i(P_i + P_0)$, $Q_{\breve{\mathcal{M}}} = \sum_{i=1}^{r} \breve{\mathcal{M}}_i(Q_i + Q_0)$. The observer gains are $\bar{L}_i$, $\breve{L}_i$, P_i, Q_i $\ i = 1, ..., r$. Hence, the estimation error $e_{\xi}(t) = \hat{\xi}(t) - \xi(t)$ has an ISS property with respect to $\Delta_{\xi_i}(t)$, and converges to a centered ball region.

Proof 1. To prove this theorem, let's consider the following fuzzy Non-Quadratic Lyapunov function (NQLF) candidate

$$V(e) = \begin{bmatrix} e_{\xi_1} \\ e_{\xi_2} \end{bmatrix}^T \begin{pmatrix} P_{\hat{\mu}} & 0 \\ 0 & Q_{\hat{\mu}} \end{pmatrix} \begin{bmatrix} e_{\xi_1} \\ e_{\xi_2} \end{bmatrix} \tag{20}$$

$$P_{\hat{\mu}} = \sum_{i=1}^{r} \mu_i(\hat{\vartheta}_x) P_i \ \text{ and } \ Q_{\hat{\mu}} = \sum_{i=1}^{r} \mu_i(\hat{\vartheta}_y) Q_i \tag{21}$$

with $P_i = P_i^T > 0$ and $Q_i = Q_i^T > 0$ are symmetric positive definite, $\mu_i(\hat{\vartheta}_k)$ satisfy (8), the NQLF $V(e(t))$ is positive too and shares the same fuzzy sets in premise parts.

Remark 3. The NQLF is a convex fuzzy rich function made up of multiple quadratic lyapunov functions (QLFs) and is more compatible with the polytopic systems from the structural viewpoint. This function introduces some degrees of freedom thanks to the matrices (P_i, Q_i) and consequently the obtained stability results may be less conservative.

Taking the derivative of 20 along the estimation error

$$\begin{aligned} \dot{V}(e) &= \dot{e}_{\xi_1}^T P_{\hat{\mu}} e_{\xi_1} + \dot{e}_{\xi_2}^T Q_{\hat{\mu}} e_{\xi_2} + e_{\xi_1}^T P_{\hat{\mu}} \dot{e}_{\xi_1} + e_{\xi_2}^T Q_{\hat{\mu}} \dot{e}_{\xi_2} \\ &+ e_{\xi_1}^T \dot{P}_{\hat{\mu}} e_{\xi_1} + e_{\xi_2}^T \dot{Q}_{\hat{\mu}} e_{\xi_2} \end{aligned} \tag{22}$$

Considering $\bar{\Gamma}_{\hat{\mu}} = \bar{\Phi}_{\hat{\mu}}^T P_{\hat{\mu}} + P_{\hat{\mu}}\bar{\Phi}_{\hat{\mu}}$, $\breve{\Gamma}_{\hat{\mu}} = \breve{\Phi}_{\hat{\mu}}^T Q_{\hat{\mu}} + Q_{\hat{\mu}}\breve{\Phi}_{\hat{\mu}}$, and applying Lemma (1), inequality (22) yields

$$\begin{aligned} \dot{V}(e) &< e_{\xi_1}^T(\Gamma_{\hat{\mu}} + P_{\hat{\mu}}\bar{D}_{\hat{\mu}}\mathcal{G}_1\bar{D}_{\hat{\mu}}^T P_{\hat{\mu}} + P_{\hat{\mu}}\mathcal{F}_1 P_{\hat{\mu}} + \mathcal{G}_2^{-1} + \dot{P}_{\hat{\mu}})e_{\xi_1} \\ &+ e_{\xi_2}^T(\breve{\Gamma}_{\hat{\mu}} + Q_{\hat{\mu}}\breve{D}_{\hat{\mu}}\mathcal{G}_2\breve{D}_{\hat{\mu}}^T Q_{\hat{\mu}} + Q_{\hat{\mu}}\mathcal{F}_2 Q_{\hat{\mu}} + \mathcal{G}_1^{-1} + \dot{Q}_{\hat{\mu}})e_{\xi_2} \\ &+ \Delta_{\xi_1}^T\mathcal{F}_1^{-1}\Delta_{\xi_1} + \Delta_{\xi_2}^T\mathcal{F}_2^{-1}\Delta_{\xi_2} \end{aligned} \tag{23}$$

($\mathcal{G}_1$, $\mathcal{G}_2$) and ($\mathcal{F}_1$, $\mathcal{F}_2$) are positive matrices.

Remark 4. Notice that $\dot{V}(e(t))$ involves the appearance of membership functions derivatives. Exploring the convexity of weighting function and adding slack matrices P_0 and Q_0 permit to transformed this parameter-dependent derivatives in (23) into a finite set in LMIs constraints in order to achieve

more relaxed stabilization conditions. A similar idea has been presented in [19], [5] on conservatism relaxation.

Lemma 2. The derivatives of $P_{\hat{\mu}}$ and $Q_{\hat{\mu}}$ are given by $\dot{P}_{\hat{\mu}} = \sum_{i=1}^{r} \dot{\mu}_i(\hat{\vartheta}_x)P_i$ and $\dot{Q}_{\hat{\mu}} = \sum_{i=1}^{r} \dot{\mu}_i(\hat{\vartheta}_y)Q_i$. There exists positive scalars $\bar{\mathcal{M}}_i$ and $\breve{\mathcal{M}}_i$ such that the weighting functions derivatives are bounded as [19]

$$|\dot{\mu}_i(\hat{\vartheta}_x)| \leq \bar{\mathcal{M}}_i \text{ and } |\dot{\mu}_i(\hat{\vartheta}_y)| \leq \breve{\mathcal{M}}_i \tag{24}$$

μ_i verify the convex sum properties (8), it obviously follows

$$\sum_{i=1}^{r} \dot{\mu}_i(\vartheta_k) = 0 \rightarrow \sum_{i=1}^{r} |\dot{\mu}_i(\hat{\vartheta}_i)| = 0 \tag{25}$$

For any symmetric slack matrices P_0 and Q_0 introducing an additional degree of freedom [19], [17], from (25) it follows

$$\sum_{i=1}^{r} |\dot{\mu}_i(\hat{\vartheta}_x)|P_0 = 0, \quad \sum_{i=1}^{r} |\dot{\mu}_i(\hat{\vartheta}_y)|Q_0 = 0 \tag{26}$$

With assumption (24), $\dot{P}_{\hat{\mu}}, \dot{Q}_{\hat{\mu}}$ are bounded as [19]

$$\dot{P}_{\hat{\mu}} = \sum_{i=1}^{r} \dot{\mu}_i(\hat{\vartheta}_x)(P_i + P_0) \leq \sum_{i=1}^{r} \bar{\mathcal{M}}_i(P_i + P_0) \tag{27}$$

$$\dot{Q}_{\hat{\mu}} = \sum_{i=1}^{r} \dot{\mu}_i(\hat{\vartheta}_y)(Q_i + Q_0) \leq \sum_{i=1}^{r} \breve{\mathcal{M}}_i(Q_i + Q_0) \tag{28}$$

Theorem 2. [19] The QLIF observer (12) is stable if the following constraints are satisfied

$$P_i = P_i^T > 0, \quad Q_i = Q_i^T > 0, \quad i = \{1, 2, .., r\} \tag{29}$$

$$P_i + P_0 \geq 0, \quad Q_i + Q_0 \geq 0 \tag{30}$$

$$\bar{\Xi}_{\hat{\mu}} = P_{\bar{\mathcal{M}}} + (\bar{\Gamma}_{\hat{\mu}} + P_{\hat{\mu}}\bar{D}_{\hat{\mu}}\mathcal{G}_1\bar{D}_{\hat{\mu}}^T P_{\hat{\mu}} + P_{\hat{\mu}}\mathcal{F}_1 P_{\hat{\mu}} + \mathcal{G}_2^{-1}) < 0 \tag{31}$$

$$\breve{\Xi}_{\hat{\mu}} = Q_{\breve{\mathcal{M}}} + \breve{\Gamma}_{\hat{\mu}} + Q_{\hat{\mu}}\breve{D}_{\hat{\mu}}\mathcal{G}_2\breve{D}_{\hat{\mu}}^T Q_{\hat{\mu}} + Q_{\hat{\mu}}\mathcal{F}_2 Q_{\hat{\mu}} + \mathcal{G}_1^{-1} < 0 \tag{32}$$

where $P_{\bar{\mathcal{M}}} = \sum_{i=1}^{r} \bar{\mathcal{M}}_i(P_i + P_0)$, $Q_{\breve{\mathcal{M}}} = \sum_{i=1}^{r} \breve{\mathcal{M}}_i(Q_i + Q_0)$, $\bar{\mathcal{M}}_i$, $\breve{\mathcal{M}}_i$, are scalars, and $P_0 = P_0^T$, $Q_0 = Q_0^T$.

Then, the $\dot{V}(e)$ is bounded as follows

$$\dot{V}(e) < e_{\xi_1}^T \bar{\Xi}_{\hat{\mu}} e_{\xi_1} + e_{\xi_2}^T \breve{\Xi}_{\hat{\mu}} e_{\xi_2} + \Delta_{\xi_1}^T \mathcal{F}_1^{-1} \Delta_{\xi_1} + \Delta_{\xi_2}^T \mathcal{F}_2^{-1} \Delta_{\xi_2} \tag{33}$$

Replacing the suitable terms, and by adding and subtracting the term $\alpha e_\xi^T \mathcal{Q}_{\hat{\mu}} e_\xi$ ($\mathcal{Q}_{\hat{\mu}} = diag(P_{\hat{\mu}}, Q_{\hat{\mu}})$) , with α is a positive scalar, the inequality (33) is equivalent to

$$\dot{V}(t) \leq \begin{bmatrix} e_{\xi_1} \\ e_{\xi_2} \end{bmatrix}^T \Psi \begin{bmatrix} e_{\xi_1} \\ e_{\xi_2} \end{bmatrix} - \alpha \underbrace{e_\xi(t)^T \mathcal{Q}_{\hat{\mu}} e_\xi(t)}_{V(e)} + \Delta_\xi^T \mathcal{F} \Delta_\xi \tag{34}$$

$$\Psi = \begin{bmatrix} \bar{\Xi}_{\hat{\mu}} + \alpha P_{\hat{\mu}} & 0 \\ 0 & \breve{\Xi}_{\hat{\mu}} + \alpha Q_{\hat{\mu}} \end{bmatrix} \tag{35}$$

with $\mathcal{F} = diag(\mathcal{F}_1^{-1}, \mathcal{F}_2^{-1})$, $\Delta_\xi = [\Delta_{\xi_1}^T, \Delta_{\xi_2}^T]^T$. The negativity of $V(e(t))$ is ensured if $\Psi < 0$. Hence, replacing (31), (32) in (35) lead to the following optimization problem

$$\bar{\Gamma}_{\hat{\mu}} + P_{\hat{\mu}}\bar{D}_{\hat{\mu}}\mathcal{G}_1\bar{D}_{\hat{\mu}}^T P_{\hat{\mu}} + P_{\hat{\mu}}\mathcal{F}_1 P_{\hat{\mu}} + \mathcal{G}_2^{-1} + \alpha P_{\hat{\mu}} + P_{\bar{\mathcal{M}}} < 0 \tag{36a}$$

$$\breve{\Gamma}_{\hat{\mu}} + Q_{\hat{\mu}}\breve{D}_{\hat{\mu}}\mathcal{G}_2\breve{D}_{\hat{\mu}}^T Q_{\hat{\mu}} + Q_{\hat{\mu}}\mathcal{F}_2 Q_{\hat{\mu}} + \mathcal{G}_1^{-1} + \alpha Q_{\hat{\mu}} + Q_{\breve{\mathcal{M}}} < 0 \tag{36b}$$

The two inequalities are connected by $\mathcal{G}_1$ and $\mathcal{G}_2$. Using Schur's complement Lemma [20], (36a) and (36b) yield to

$$\begin{bmatrix} \bar{\Gamma}_{\hat{\mu}} + \mathcal{G}_2^{-1} + \alpha P_{\hat{\mu}} + P_{\bar{\mathcal{M}}} & P_{\hat{\mu}}\bar{D}_{\hat{\mu}} + P\hat{\mu}\mathcal{F}_1 \\ \bar{D}_{\hat{\mu}}^T P_{\hat{\mu}} + \mathcal{F}_1^T P_{\hat{\mu}} & -\mathcal{G}_1^{-1} \end{bmatrix} < 0$$
$$\begin{bmatrix} \breve{\Gamma}_{\hat{\mu}} + \mathcal{G}_1^{-1} + \alpha Q_{\hat{\mu}} + Q_{\breve{\mathcal{M}}} & Q_{\hat{\mu}}\breve{D}_{\hat{\mu}} + Q_{\hat{\mu}}\mathcal{F}_2 \\ \breve{D}_{\hat{\mu}}^T Q_{\hat{\mu}} + \mathcal{F}_2^T Q_{\hat{\mu}} & -\mathcal{G}_2^{-1} \end{bmatrix} < 0 \tag{37}$$

By using the convex sum propriety, the definitions of the matrices $\bar{\Gamma}_{\hat{\mu}}$ and $\breve{\Gamma}_{\hat{\mu}}$ and change of variables ($\Omega_1 = \mathcal{G}_1^{-1}$, $\Omega_2 = \mathcal{G}_2^{-1}$) and ($\bar{R}_i = P_i\mathcal{F}_1$, $\breve{R}_i = Q_i\mathcal{F}_2$), (37) are equivalent to the relaxed LMI conditions (19a) and (19b) in theorem 1. The conservativeness issues can further counterbalanced, for instant, by using some decoupling lemmas like Tuan's lemma [21] or Finsler's lemma [22]. Another more relaxed approach called the Polya's theorem is based on expanding the degree of fuzzy summations to increase the degree of freedom [23], [22]. It is easy to derive conditions (18) in the theorem 1.

C. Stability Analysis

Now, if $\Psi < 0$, then (34) can be bounded as follows

$$\dot{V}(t) \leq -\alpha V(t) + \Delta_\xi^T \mathcal{F} \Delta_\xi \tag{38}$$

By integrating (38) over the interval $[0, t]$, we get

$$V(t) \leq V(0)e^{-\alpha t} + \frac{\mathcal{F}}{\alpha} \|\Delta_\xi(s)\|_\infty^2 \tag{39}$$

Knowing that $V(t)$ is a Lyapunov function, it can be bounded by $\lambda_{\min} \|e_\xi(t)\|_2^2$ and $\lambda_{\max} \|e_\xi(t)\|_2^2$, where $\lambda_{\min}$ and $\lambda_{\max}$ are the eigenvalues of the matrices $\mathcal{Q}_{\hat{\mu}} = diag(P_{\hat{\mu}}, Q_{\hat{\mu}})$. Assuming that $\chi_1 I \leq \mathcal{Q}_{\hat{\mu}} \leq \chi_2 I$, with ($\chi_1 \leq \lambda_{min}(\mathcal{Q}_{\hat{\mu}})$ and $\lambda_{max}(\mathcal{Q}_{\hat{\mu}}) \leq \chi_2$), it obviously follows that

$$\chi_1 ||e(t)|| \leq V(e(t)) \leq \chi_2 ||e(t)|| \tag{40}$$

Under this condition, the state estimation error is reduced to

$$\|e_\xi(t)\|_2 \leq \varphi_1 \|e_\xi(0)\|_2 e^{-\frac{\alpha}{2}t} + \varphi_2 \|\Delta_\xi(t)\|_\infty \tag{41}$$
$$\varphi_1 = \sqrt{\frac{\lambda_{\max}(\mathcal{Q}_{\hat{\mu}})}{\chi_1}}, \varphi_2 = \sqrt{\frac{\lambda_{\max}(\mathcal{Q}_{\hat{\mu}})}{\gamma}}, \quad \gamma = \frac{\alpha\chi_1}{\mathcal{F}}$$

Hence, when $t \rightarrow \infty$ the exponential converge to zero with the minimal ISS gain φ_2, implies $\lim_{t\rightarrow\infty} \|e_\xi\|_2 < \varphi_2 \max(\|\Delta_\xi\|_\infty)$.

Remark 5. The stability of pseudo-disturbed TS system affected by the mismatching terms or unmeasured nonlinearities, have been widely investigated, by exploiting the Lipschitz hypotheses [24], nonlinear consequents [25], ISS propriety [17], or immersion techniques [26], etc. It is known that ISS results guarantee the system robustness and provide LMIs without needing any calculation of the Lipschitz constant or any new coordinates generation from auxiliary dynamics.

From the boundedness of $\Delta_{\xi(t)}$ and thanks to definition (1), it is shown that the error dynamics verifies the ISS property. Therefore, minimizing the ISS gain is equivalent to minimize positive scalars $\eta = diag(\eta_1, \eta_2)$. Hence, the chosen cost function is a linear combination given in (17) in theorem 1. Assuming $\lambda_{\min}(\mathcal{Q}_i) \geq \chi_1$ ($\mathcal{Q}_i > \chi_1 I$), one obtains

$$\sqrt{\frac{\lambda_{\max}(\mathcal{Q}_i)}{\gamma}} \leq \sqrt{\eta} \rightarrow (\gamma\eta)^2 I - \mathcal{Q}_i^T \mathcal{Q}_i > 0 \tag{42}$$

By applying the Schur's complement lemma [9] , inequality (42) is written as the LMI constraint (19c).

Remark 6. The choice of $\mathcal{Q}_i = \{P_i, Q_i\}$ providing a small set of convergence is constrained by assuming $\lambda_{\min}(\mathcal{Q}_i) \geq \chi_1$ ($\mathcal{Q}_i > I\chi_1$). This assumption may introduce some conservatism. However, since the main aim here is to find the minimal ISS gain, the proposed reasoning is sufficient. This optimization step has been tested intensively [27], a similar

ISS result was established for LPV systems. The procedure to solve this optimization problem begins by imposing α and χ_1, $\mathcal{F}$ (so γ) before solving the LMIs (19a-19c). If, no solution is found, one has to decrease γ or χ_1.

D. Observer sensitivity and robustness proof

Consider the following LPV interconnected uncertain system affected by disturbances

$$\dot{\xi} = \underbrace{\begin{bmatrix} \bar{A}_\mu + \Delta\bar{A}_\mu & 0 \\ 0 & \breve{A}_\mu + \Delta\breve{A}_\mu \end{bmatrix}}_{\mathcal{A}_\mu + \Delta\mathcal{A}_\mu} \xi + \underbrace{\begin{bmatrix} \bar{B}_\mu + \Delta\bar{B}_\mu & 0 \\ 0 & \breve{B}_\mu + \Delta\breve{B}_\mu \end{bmatrix}}_{\mathcal{B}_\mu + \Delta\mathcal{B}_\mu} u + \begin{bmatrix} 0 & \bar{D}_\mu \\ \breve{D}_\mu & 0 \end{bmatrix} \xi + \underbrace{\begin{bmatrix} \bar{\varpi} & 0 \\ 0 & \breve{\varpi} \end{bmatrix}}_{\varpi(t)} \tag{43}$$

$$y = \begin{bmatrix} \bar{C} & 0 \\ 0 & \breve{C} \end{bmatrix} \xi + \underbrace{\begin{bmatrix} \bar{\Omega} & 0 \\ 0 & \breve{\Omega} \end{bmatrix}}_{\Omega(t)}$$

The estimation error derivative $\dot{e}_\xi$ becomes

$$\dot{e}_\xi = \begin{bmatrix} \bar{\Phi}_{\hat{\mu}} & \bar{D}_{\hat{\mu}} \\ \breve{D}_{\hat{\mu}} & \breve{\Phi}_{\hat{\mu}} \end{bmatrix} \times e_\xi + \begin{bmatrix} \Delta_{\Delta\xi_1} \\ \Delta_{\Delta\xi_2} \end{bmatrix} \tag{44}$$

$$\begin{aligned} \Delta_{\Delta\xi_1} &= \Delta_{\xi_1} + \Delta\bar{A}_\mu\xi_1 + \Delta\bar{B}_\mu u_B + \bar{\vartheta}(t) + P_{\hat{\mu}}^{-1}\bar{L}_i\bar{\Omega}(t) \\ \Delta_{\Delta\xi_2} &= \Delta_{\xi_2} + \Delta\breve{A}_\mu\xi_2 + \Delta\breve{B}_\mu u_\delta + \breve{\vartheta}(t) + Q_{\hat{\mu}}^{-1}\breve{L}_i\breve{\Omega}(t) \end{aligned}$$

The errors' dynamic (44) is similar to that obtained in (13). The difference lies in the perturbation vectors ($\Delta_{\Delta\xi_1}(t)$, $\Delta_{\Delta\xi_2}(t)$) which includes the uncertain matrices $\Delta\bar{A}_\mu, \Delta\breve{A}_\mu$, $\Delta\bar{B}_\mu, \Delta\breve{B}_\mu$, and the bounded disturbances ϖ and Ω defining the measurement noise and perturbations on the system. In the uncertain case, the estimation error will be bounded as

$$\begin{aligned} \|e_\xi(t)\|_2 \quad &\leq \quad \varphi_1 \|e_\xi(0)\|_2 e^{-\frac{\alpha t}{2}} + \varphi_2 \|\Delta_\xi(t)\|_\infty \\ &+ \quad \varphi_2 \left\|\Delta\mathcal{A}_\mu\xi(t) + \Delta\mathcal{B}_\mu u(t) + \varpi(t) + \mathcal{Q}_{\hat{\mu}}^{-1} L_i \Omega(t)\right\|_\infty \end{aligned}$$

When $t \to \infty$, the estimation error will be bounded in the nominal case by the quantity $\varphi_2 \|\Delta(t)\|_\infty$, and by the $\varphi_2 \left(\|\Delta_\xi(t)\|_\infty + \left\|\Delta\mathcal{A}_\mu\xi(t) + \Delta\mathcal{B}_\mu u(t) + \varpi(t) + \mathcal{Q}_{\hat{\mu}}^{-1} L_i \Omega(t)\right\|_\infty\right)$, in the uncertain case. Consequently, the observer accuracy will be better in the nominal case because the convergence bounds are smaller. Note that all the uncertainties are included in the disturbance-like term. This fact allows to use the robust observer result in Section IV and hence to prove the ISS.

V. Experimental Results and Discussions

In this section, an assessment of the QLIF observer is presented using hardware experiments under real-world driving maneuvers. To this end, the dynamic driving SHERPA (French Acronym for "Simulateur Hybride d'Etude et de Recherche de PSA Peugeot Citroen pour l'Automobile") simulator is used [5]. It includes a full car mock-up Peugeot 206 vehicle installed on a six-DoF platform, presented in Fig. 3a.

A. Observer Evaluation in Real-World Conditions

The real-world test scenario, acquired using the SHERPA car simulator, was performed on a Satory test track. This test track is an urban scenic road performed in accordance with a real regular driving condition and good environmental conditions. It allows to highlight the observer performance by covering a broad spectrum of the vehicle dynamics within and beyond its linearization domain. According to safety and comfort margins and through our own experimentation in the simulator, the following bounds are considered $0.001 \leq v_x \leq 30[m/s]$, $-0.5 \leq v_y \leq 1.5[m/s]$, $|\sin(\delta)| \leq 1$, $|\cos(\delta)| \leq 1$, $-1 \leq \Delta_v \leq 1$, $0.001 \leq \varrho_f \leq 220$, $0.001 \leq \varrho_r \leq 200$.

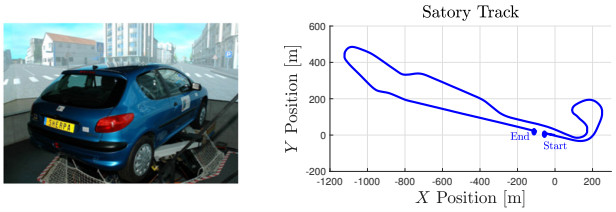

(a) SHERPA driving simulator. (b) X-Y positions.

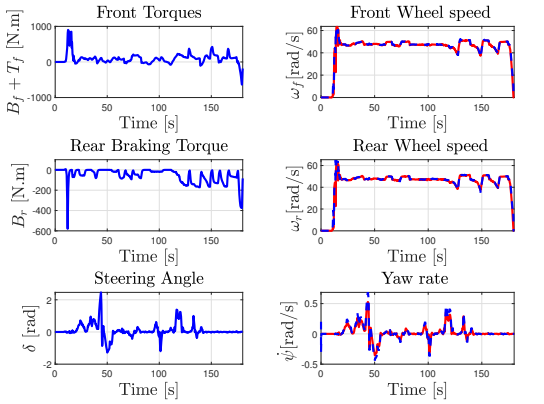

(c) Braking, traction torques and steerig angle inputs. (d) SHERPA data (red) and estimated (dashed blue).

Fig. 3: Satory test track in SHERPA-LAMIH driving simulator

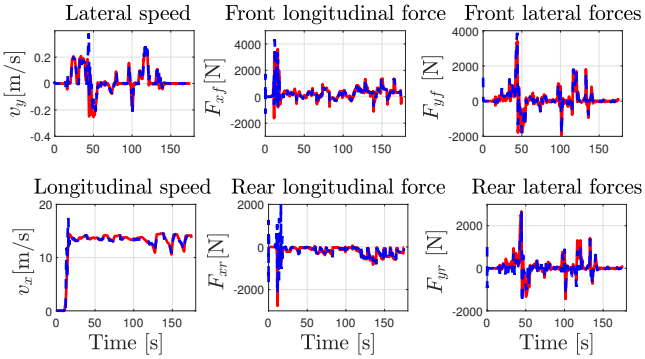

Fig. 4: Estimation performance: SHERPA (red) and observer (blue).

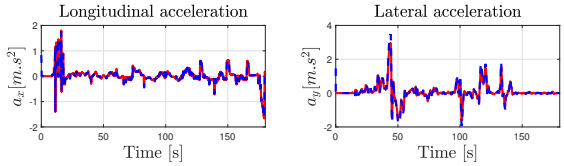

Fig. 5: Validation performance for Satory test track.

The chosen parameters are $\alpha = 0.01$, $\mathcal{F} = 5$, $\chi_1 = 1$ and $a = 0.9$. As depicted in Fig. 3b, the road track is composed of straight lines followed by several curved profiles including narrow turns and big bends. Hence, the vehicle system requires: the two braking torques on both front and rear wheels applied to reduce the longitudinal speed, the traction torque T_f applied on the front wheel, involving also a medium hard steering angle input applied on the lateral model. These inputs are represented in Fig. 3c. In Fig. 3d, estimated yaw rate and angular velocities profiles are compared to

their respective measurements provided by the car simulator software. Since these states variables are measured and used in the observer design, the state estimation demonstrates a finite-time estimation convergence. On the other hand, Fig. 4 reports the estimation results of unmeasured state variables namely the lateral and longitudinal speeds v_y, v_x, the front/rear lateral F_{yf}, F_{yr} and longitudinal F_{xf}, F_{xr} forces. The longitudinal speed is an unmeasured time-varying parameter ranging from $0.001m/s$ to $20m/s$ as shown in Fig. 4. It can be seen that the observer has a rapid dynamic transition and good performance are guaranteed for simultaneous longitudinal and lateral states dynamics estimation even for an aggressive driving maneuver in a too tight bend which excites the vehicle away from the straight-line dynamics. The small differences between the estimate and the actual (SHERPA), especially, at the peak of the forces, is due, mainly, to the fact that the simulator aims to compensates the coupling effect on the forces, which is not the case of our model. This can be explained by modeling errors due to linearization, among other reasons, of the huge steer angle. Consequently, the ISS performances are still guaranteed and the tire forces and speeds are well estimated. For validation, the estimation of unmeasured states (F_{x_i}, F_{y_i}) are used to reconstruct the lateral and longitudinal accelerations a_y, a_x at the center of gravity CoG by using the two equations: $\hat{a}_y = \frac{(\hat{F}_{yf}+\hat{F}_{yr})}{m}$ and $\hat{a}_x = \frac{(\hat{F}_{xf}+\hat{F}_{xr})}{m}$. Fig. 5 represents the estimated cornering and longitudinal accelerations and the corresponding one given by the car driving simulator. Once again, the acceleration estimation demonstrates a finite-time estimation convergence. Despite modeling assumptions, it can be appreciated that the proposed observer provides a good estimation accuracy under highly dynamic maneuvering, and small estimation errors with ISS performances.

B. Observer Robustness and sensitivity

The observer was designed with the nominal default parameters, road friction coefficient of $\mu = 1$ (dry asphalt) and ideal sensors. To asses the sensitivity and robustness, the observer will be excited with a measurements' noise then tested against parameters uncertainties and regarding road friction changes. The same digital database of the Satory test track presented in Section V, Fig. 3b is considered. Firstly, we assume a centered and random noises with $5-10\%$ of the maximal measured values. The resulting observer performances are depicted in Fig. 6. It can be noted that the effect of the noise on the states estimation is limited, however, it remains barely visible. Secondly, the observer robustness is evaluated against parameters uncertainties. We consider that the vehicle mass with driver has undergone a variation of $\pm 300kg$ on the design values. Finally, the observer sensitivity is tested with respect to the road friction variation. To this end, two cases (moderately wet road $\mu = 0.6$ and very wet road $\mu = 0.4$) are considered. The effect of the over or the underweight, the road friction changes and the noise influence are evaluated using statistics indexes. To this end, the estimation are compared with their counterparts in table I by means of the root mean square error ($\text{RMSE}_{\%}$), mean square error percentage ($\text{MSE}_{\%}$) and normalized mean square error ($\text{NMSE}_{\%}$)

$$\text{MSE}_{\%} = \frac{100\,\|y-\hat{y}\|^2}{N_{dataset}}, \quad \text{NMSE}_{\%} = 100 - \frac{100(\|y-\hat{y}\|^2)}{\|y-\text{mean}(y)\|^2}$$
$$\text{RMSE}_{\%} = 100\sqrt{\frac{1}{N_{\text{dataset}}}\sum_{i=1}^{N_{\text{dataset}}}(y-\hat{y})^2}, \; N_{\text{dataset}}\text{: data points length} \quad (45)$$

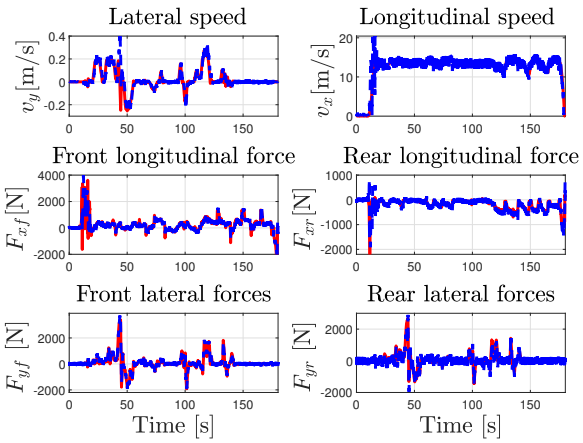

Fig. 6: Observer robustness against sensors' noise.

From Table I, the observer gives the better estimation for the nominal case (A) where the maximal values of ($\text{MSE}_{\%}$, $\text{RMSE}_{\%}$) are the lowest and $\text{NMSE}_{\%}$ are the largest. As expected, the estimation errors increase when the vehicle mass or the road adherence changes and becomes more important in the case where the noise effect is considered with a maximum degradation of (9%). However, even with degradation, these errors are always lowers than $\text{MSE}_{\%} < 7.5\%$ which confirms that the performances of the observer are preserved. Indeed, even with mass variations, road surface uncertainties and noise consideration, the deviations amplitude of the errors is quantified with a value less than $\text{RMSE}_{\%} < 12.3\%$, and $NMSE_{\%} > 84.7\%$. To conclude, the quantification results clearly confirm that QLIF observer is robust enough to handle the noisy case, road friction variation and parameters uncertainties and QLIF still have good ISS performances.

VI. CONCLUSION

This paper presents a QLIF observer synthesis for *simultaneous* estimation of the lateral and longitudinal vehicle dynamics. The outlined observer is designed considering Quasi-LPV vehicle interconnected model taking into account real constraints such as the variations in the immeasurable longitudinal and lateral speed, non-linearities of steering angle and the tire slip velocities during the interconnected-sub observers design. The result is formalized using NQLF Lyapunov function and more relaxed stabilisation condition (Polya's theorem) where the observer's gains are computed with less restrictive stability conditions and conservativeness by resolving an LMIs optimization problem aiming to minimize the estimation error bound based on ISS propriety. The observer is evaluated based on a set of nominal parameters exactly known and in the presence of ideal sensors (no-noise) using a "full scale" SHERPA car simulator under real-world driving situation. The effectiveness is highlighted with error quantification under noise consideration, regarding road friction changes and parameters uncertainties. For future works, the proposed observer will be validated experimentally in real-time using the DS7 prototype vehicle which is being instrumented with the various sensors required to measure the longitudinal and lateral dynamics of the vehicle.

TABLE I: Case (A) represents the nominal case: $\mu_1 = 1$, robustness to vehicle mass in: case (B): $M^+ = M + 300$, case (C): $M^- = M - 300$, case (D) considers the noise effect, robustness to road friction in case (E): $\mu_2 = 0.6$ and case (F): $\mu_3 = 0.4$.

	$\dot{\psi}$			ω_f			ω_r			a_x			a_y		
	MSE	**RMS**	**NMSE**	**MSE**	**RMS**	**NMSE**	**MSE**	**RMS**	**NMSE**	**MSE**	**RMS**	**NMSE**	**MSE**	**RMS**	**NMSE**
$(\boldsymbol{A})$	0.057	2.42	95.81	3.07	9.31	97.64	4.08	10.13	95.52	0.023	1.66	98.93	2.78	5.57	91.85
$(\boldsymbol{B})$	0.059	2.34	95.74	3.26	10.34	96.38	5.54	10.92	92.68	2.14	5.08	98.86	2.67	5.85	90.75
$(\boldsymbol{C})$	0.061	2.38	95.68	3.35	10.41	95.82	4.74	11.61	93.97	2.68	5.76	97.95	2.84	6.27	89.12
$(\boldsymbol{D})$	0.219	4.13	90.47	5.36	12.18	91.24	7.28	11.89	89.64	2.87	7.19	90.11	4.34	8.26	85.34
$(\boldsymbol{E})$	0.087	2.59	94.61	3.69	10.71	96.17	5.69	12.05	93.79	2.91	7.12	96.41	3.48	7.22	88.18
$(\boldsymbol{F})$	0.132	2.96	90.53	4.38	11.86	91.03	6.29	12.25	93.62	2.94	7.21	94.24	3.79	7.55	84.75

TABLE II: System's parameters description.

Parameter	Description
v_y, v_x	Lateral and longitudinal velocities ($m.s^{-1}$).
$\dot{\psi}$, δ	Yaw rate ($rad.s^{-1}$) and Steering angle (rad).
ω_f, ω_r	Angular velocities of the front and rear wheels ($rad.s^{-1}$).
F_{yi}, F_{xi}	Cornering and Longitudinal forces (N).
B_i, T_i	Braking torques and Engine torque ($N.m$).
m, I_z	Vehicle mass (kg), inertia about the z-axis ($kg.m^2$)
C_α, C_λ	Cornering and longitudinal stiffness parameters ($N.rad^{-1}$)
i_{iy}, R	Wheels moment of inertia ($kg.m^2$) and rolling radius (m).
l_f, l_r	Distances between the C.G. and front and rear axles (m)
C_x, C_y	Aerodynamic drag coefficients
Numerical values	
$C_{\lambda_f} = 71165$; $C_{\lambda_r} = 62671$; $C_{\alpha_f} = 57000$; $C_{\alpha_r} = 59000\ N.rad^{-1}$	
$m = 2500kg$ $R = 0.313\ m$ $l_f = 1.3\ l_r = 1.6\ m$ $h = 0.76\ m$	
$I_z = 2800\ kg.m^2$ $i_{ry} = i_{fy} = 10\ kg.m^2$ $\sigma = 0.24$ $C_x = 0.25$	

REFERENCES

[1] K. Han, E. Lee, M. Choi, and S. B. Choi, "Adaptive scheme for the real-time estimation of tire-road friction coefficient and vehicle velocity," *IEEE/ASME Transactions on Mechatronics*, vol. 22, no. 4, pp. 1508–1518, 2017.

[2] S. Zhou, H. Zhao, W. Chen, Z. Liu, H. Wang, and Y. Liu, "Dynamic state estimation and control of a heavy tractor-trailers vehicle," *IEEE/ASME Transactions on Mechatronics*, 2020.

[3] N. M'sirdi, A. Rabhi, N. Zbiri, and Y. Delanne, "Vehicle–road interaction modelling for estimation of contact forces," *Vehicle System Dynamics*, vol. 43, no. sup1, pp. 403–411, 2005.

[4] M. Boufadene, M. Belkheiri, A. Rabhi, and A. E. Hajjaji, "Vehicle longitudinal force estimation using adaptive neural network nonlinear observer," *International Journal of Vehicle Design*, vol. 79, no. 4, pp. 205–220, 2019.

[5] A.-T. Nguyen, T.-M. Guerra, C. Sentouh, and H. Zhang, "Unknown input observers for simultaneous estimation of vehicle dynamics and driver torque: Theoretical design and hardware experiments," *IEEE/ASME Transactions on Mechatronics*, vol. 24, no. 6, pp. 2508–2518, 2019.

[6] M. Fouka, L. Nehaoua, D. Ichalal, H. Arioui, and S. Mammar, "Road geometry and steering reconstruction for powered two wheeled vehicles," in *2018 21st International Conference on Intelligent Transportation Systems (ITSC)*. IEEE, 2018, pp. 2024–2029.

[7] M. Fouka, L. Nehaoua, M. Dabladji, H. Arioui, and S. Mammar, "Adaptive observer for motorcycle state estimation and tire cornering stiffness identification," in *2018 IEEE Conference on Decision and Control (CDC)*. IEEE, 2018, pp. 3018–3024.

[8] W. Han, L. Xiong, and Z. Yu, "Interconnected pressure estimation and double closed-loop cascade control for an integrated electro-hydraulic brake system," *IEEE/ASME Transactions on Mechatronics*, 2020.

[9] M. Fouka, L. Nehaoua, H. Arioui, and S. Mammar, "Interconnected observers for a powered two-wheeled vehicles: Both lateral and longitudinal dynamics estimation," in *2019 IEEE 16th International Conference on Networking, Sensing and Control (ICNSC)*. IEEE, 2019, pp. 163–168.

[10] R. A. Cordeiro, A. C. Victorino, J. R. Azinheira, P. A. Ferreira, E. C. de Paiva, and S. S. Bueno, "Estimation of vertical, lateral, and longitudinal tire forces in four-wheel vehicles using a delayed interconnected cascade-observer structure," *IEEE/ASME Transactions on Mechatronics*, vol. 24, no. 2, pp. 561–571, 2019.

[11] T. Boukhobza, F. Hamelin, S. Martinez-Martinez, and D. Sauter, "Structural analysis of the partial state and input observability for structured linear systems: Application to distributed systems," *European Journal of Control*, vol. 15, no. 5, pp. 503–516, 2009.

[12] T. M. Guerra, V. Estrada-Manzo, and Z. Lendek, "Observer design for takagi–sugeno descriptor models: An lmi approach," *Automatica*, vol. 52, pp. 154–159, 2015.

[13] R. Rajamani, *Vehicle dynamics and control*. Springer Science & Business Media, 2011.

[14] V. V. Vantsevich and J. P. Gray, "Relaxation length review and time constant analysis for agile tire dynamics control," in *International Design Engineering Technical Conferences and Computers and Information in Engineering Conference*, vol. 57106. American Society of Mechanical Engineers, 2015, p. V003T01A038.

[15] K. Tanaka and H. O. Wang, *Fuzzy control systems design and analysis: a linear matrix inequality approach*. John Wiley & Sons, 2004.

[16] A.-T. Nguyen, C. Sentouh, and J.-C. Popieul, "Driver-automation cooperative approach for shared steering control under multiple system constraints: Design and experiments," *IEEE Transactions on Industrial Electronics*, vol. 64, no. 5, pp. 3819–3830, 2016.

[17] D. Ichalal, B. Marx, J. Ragot, and D. Maquin, "Advances in observer design for takagi-sugeno systems with unmeasurable premise variables," in *2012 20th Mediterranean Conference on Control & Automation (MED)*. IEEE, 2012, pp. 848–853.

[18] J. Pan, A.-T. Nguyen, T.-M. GUERRA, and D. ICHALAL, "A unified framework for asymptotic observer design of fuzzy systems with unmeasurable premise variables," *IEEE Transactions on Fuzzy Systems*, 2020.

[19] L. A. Mozelli, R. M. Palhares, F. Souza, and E. M. Mendes, "Reducing conservativeness in recent stability conditions of ts fuzzy systems," *Automatica*, vol. 45, no. 6, pp. 1580–1583, 2009.

[20] S. Boyd, L. El Ghaoui, E. Feron, and V. Balakrishnan, *Linear Matrix Inequalities in System and Control Theory*. SIAM ed., 1994.

[21] H. D. Tuan, P. Apkarian, T. Narikiyo, and Y. Yamamoto, "Parameterized linear matrix inequality techniques in fuzzy control system design," *IEEE Transactions on fuzzy systems*, vol. 9, no. 2, pp. 324–332, 2001.

[22] A. Sala and C. Arino, "Asymptotically necessary and sufficient conditions for stability and performance in fuzzy control: Applications of polya's theorem," *Fuzzy sets and systems*, vol. 158, no. 24, pp. 2671–2686, 2007.

[23] D. Ichalal, B. Marx, D. Maquin, and J. Ragot, "New fault tolerant control strategy for nonlinear systems with multiple model approach," in *2010 Conference on Control and Fault-Tolerant Systems (SysTol)*. IEEE, 2010, pp. 606–611.

[24] P. Bergsten, R. Palm, and D. Driankov, "Observers for takagi-sugeno fuzzy systems," *IEEE Transactions on Systems, Man, and Cybernetics, Part B (Cybernetics)*, vol. 32, no. 1, pp. 114–121, 2002.

[25] H. Moodi and M. Farrokhi, "Robust observer-based controller design for takagi–sugeno systems with nonlinear consequent parts," *Fuzzy Sets and Systems*, vol. 273, pp. 141–154, 2015.

[26] D. Ichalal, B. Marx, S. Mammar, D. Maquin, and J. Ragot, "How to cope with unmeasurable premise variables in takagi–sugeno observer design: Dynamic extension approach," *Engineering Applications of Artificial Intelligence*, vol. 67, pp. 430–435, 2018.

[27] D. Ichalal, B. Marx, J. Ragot, and D. Maquin, "Unknown input observer for lpv systems with parameter varying output equation," *IFAC-PapersOnLine*, vol. 48, no. 21, pp. 1030–1035, 2015.

Majda FOUKA received the Dipl.-Ing. degree in automatic and control systems from the The National Polytechnic School, Algeria, in 2015; the M.S. degree in Automatic and application from National Higher Engineering School of Poitiers (ENSIP), France and the Ph.D. degree in automatic and automobile from the University of Evry Val d'Essonne-Paris Saclay, France, in 2019. Dr. Majda was a research assistant in IBISC Laboratory, University of Evry Val d'Essonne, France. She is currently postdoctoral researcher at the University of Valenciennes in LAMIH-UMR CNRS 8201 France. Her main research interests include automotive control, state and parameters estimation, observer design of nonlinear systems with special focus on the fields of intelligent transportation systems, human driver modeling and cooperation in shared control for assistance systems.

Chouki SENTOUH received the M.Sc. degree in automatic control from the University of Versailles, France, in 2003, and the PhD degree in automatic control from the University of Evry, France, in 2007. He was a CNRS postdoctoral researcher at the LS2N laboratory UMR CNRS 6004, Ecole Centrale de Nantes, France, from 2007 to 2009. Since 2009, he is an Associate Professor in the "Department of Automatic Control", from the LAMIH laboratory UMR CNRS 8201, Hauts-de-France Polytechnic University, France. His research fields include robust nonlinear control and observation applied to automotive control, driver assistance systems that can be characterized in accordance with level of automation and interaction with human driver, human driver modeling, conflict manage in shared control and cooperation in intelligent transportation systems.

Jean-Christophe Popieul is Professor in Automatic Control at "Université Polytechnique Hauts-de-France" in LAMIH-UMR CNRS 8201. Specialized in Human Centered Automation, he participated in many collaborative projects dealing with ADAS (Predit ARCOS, ANR ABV, ANR CoCoVeA, ANR AutoConduct ...). He is currently working on control sharing for full driving automation and is the coordinator of the ELSAT 2020 project (Haut de France transportation project 2015-2021, 350 researchers involved) and ANR CoCoVeIA. He is a member of several scientific boards (ANR, i-Trans competitivity cluster, IRT Railenium ...). In parallel with his research activity he is at the head of the Interactive Simulation Platforms of the LAMIH-CNRS: SHERPA driving simulator and PSCHITT-Rail train/tramway simulator.